Journal of Drug Delivery Science and Technology 58 (2020) 101784

Contents lists available at ScienceDirect

Journal of Drug Delivery Science and Technology

journal homepage: www.elsevier.com/locate/jddst

Praziquantel-loaded solid lipid nanoparticles: Production, physicochemical characterization, release profile, cytotoxicity and *in vitro* activity against *Schistosoma mansoni*

Luciana Nalone Andrade[a,b], Conrado Marques[a,b], Thallysson Barbosa[a,b], Rafael Santos[a,b], Marco Vinícius Chaud[b], Classius Ferreira da Silva[c], Cristiane Bani Corrêa[d], Ricardo Guimarães Amaral[d], Rogéria de Souza Nunes[d], Joyce Kelly M.C. Gonsalves[e], Silmara Allegretti[f], Eliana B. Souto[g,h,*], Patrícia Severino[a,**]

[a] Laboratory of Nanotechnology and Nanomedicine - ITP, University Tiradentes – UNIT, 49032-490, Aracaju, Sergipe, Brazil
[b] University of Sorocaba – UNISO, Laboratory of Biomaterials and Nanotechnology, Sorocaba, SP, CEP 18023-000, Brazil
[c] University of São Paulo, Laboratory of Biotechnology and Natural Products, Diadema, SP, 09913-030, Brazil
[d] Federal University of Sergipe, São Cristóvão, SE, 49100-000, Brazil
[e] Collegiate of Pharmacy, Federal University of Vale do São Francisco - UNIVASF, Petrolina, PE, 56304-917, Brazil
[f] Animal Biology Department, Institute of Biology, Estate University of Campinas (Unicamp), Campinas, 13083-862, SP, Brazil
[g] Department of Pharmaceutical Technology, Faculty of Pharmacy, University of Coimbra (FFUC), 3000-548, Coimbra, Portugal
[h] CEB – Centre of Biological Engineering, University of Minho, Campus de Gualtar, 4710-057, Braga, Portugal

ARTICLE INFO

Keywords:
Solid lipid nanoparticles
Praziquantel
Helminthiases
Schistosoma mansoni

ABSTRACT

Praziquantel (PZQ) is an anthelmintic drug, being the first choice for the treatment of schistosomiasis. Its high hydrophobic character and its low water solubility are the main limitations to the development of liquid formulations for the oral administration of the drug. The aim of this work was to develop Solid Lipid Nanoparticles (SLN) for the loading of PZQ for the treatment of *S. mansoni* infections. PZQ-SLN were produced by hot high shear homogenization. The obtained SLN exhibited a mean size of ~300 nm, with a polydispersity index of ~0.20, zeta potential of ~ -28 mV and encapsulation efficiency of 92.31%. Thermal analysis demonstrated that the production process reduced the lipid crystallinity of the SLN matrices, which displayed a spherical morphology by scanning electron microscopy (SEM). The mathematical fitting of the release profile demonstrated that PZQ followed the Weibull model whereas PZQ-loaded SLN the Peppas model. PZQ-loaded SLN were more effective in inducing *S. mansoni* death than PZQ alone. The increased drug solubility did not exhibit toxicity against human fibroblast cell lines (L929). PZQ-loaded SLN demonstrated great parasiticidal properties, being an improved alternative to the classical treatment of schistosomiasis.

1. Introduction

Schistosoma mansoni, Schistosoma japonicum, Schistosoma haematobium, Schistosoma intercalatum, and *Schistosoma mekongi* are Trematoda classes of parasites from the Schistosomatidae family, at least five from those species are known to infect humans [1]. Their geographical distribution occurs in tropical and subtropical areas within 78 countries, 52 of which exhibit endemic pattern [2]. The treatment of this disease usually follows praziquantel (PZQ) and oxamniquine (OXA) schemes [3].

Currently, PZQ is the drug of choice for schistosomiasis treatment. It is derived from pyrazine-isoquinoline, included in group II of the Biopharmaceutical Classification System (BCSII), exhibiting low water solubility and high permeability "[Pinheiro, 2014 #79]". Other limitations are the need for large dosages and unpleasant taste compromising the treatment of risky groups (e.g. children) [4].

In this context, several works have been proposing new ways to deliver these drugs and to ensure safety, quality and efficacy. Drug

* Corresponding author. Department of Pharmaceutical Technology, Faculty of Pharmacy, University of Coimbra, Pólo das Ciências da Saúde, Azinhaga de Santa Comba, 3000-548, Coimbra, Portugal.
** Corresponding author. Program in Industrial Biotechnology, Laboratory of Nanotechnology and Nanomedicine (LNMED), Institute of Technology and Research (ITP), Tiradentes University (UNIT) - Aracaju / SEA, Av. Murilo Dantas, 300, Farolândia, Aracaju, SE, CEP 49032-490, Brazil.;
E-mail addresses: ebsouto@ebsouto.pt (E.B. Souto), pattseverino@gmail.com, patricia_severino@itp.org.br (P. Severino).

https://doi.org/10.1016/j.jddst.2020.101784
Received 9 June 2019; Received in revised form 17 March 2020; Accepted 27 April 2020
Available online 15 May 2020

delivery systems at the nanoscale have been extensively applied to improve gastrointestinal drug absorption [5–7].

Solid lipid nanoparticles (SLN) holds the spotlight for lipophilic drug delivery in the biopharmaceutical field [8]. Recent studies have demonstrated that PZQ can be successfully incorporated into SLN via many production methods, but more typically hot homogenization and ultrasound methods [9–11]. The use of lipids improves the bioavailability of lipophilic drugs and promotes controlled drug release after oral administration and could be a new approach for schistosomiasis treatment.

The high physical, chemical and biological stability, the solid state of the lipid matrix of SLN under ambient and body temperatures, excellent *in vitro* and *in vivo* tolerability, biodegradability and high bioavailability combine several advantages of SLN to be used as drug carrier for PZQ. Due to its solid matrix, SLN protect PZQ from chemical and oxidative stress [1], also providing controlled release properties. Besides, several organisms show the ability to metabolise the lipid compounds used in the production of SLN.

The present work aimed at developing PZQ-loaded SLN via hot homogenization method. The *in vitro* cell viability studies were performed on L929 cells line and *in vitro* treatment assessment used *Schistosoma mansoni* adult parasites.

2. Methodology

2.1. Materials

PZQ was provided by Henrifarma® (São Paulo, Brazil). Soybean lecithin (Lipoid®S75) was purchased from Lipoid GmbH (Ludwigshafen, Germany), Tween® 20 and glycerine were bought from Synth (São Paulo, Brazil). Cetyl palmitate was donated as a gift from Croda (Campinas, Brazil). All other reagents were bought from Sigma® (Salvador, Brazil). Double-distilled water was used after filtration in a Millipore® system (home supplied).

2.2. Methods

2.2.1. Pre-formulation study

PZQ (20 mg) solubility in cetyl palmitate (1, 5 and 10%, m/m) was evaluated following the protocol as described by Chaud et al. [12], with slight modifications. The samples were heated in a thermostatic water bath (Marconi, model MA 127/BD, Brazil), for 1 h at 85 °C. Samples were then kept at room temperature until complete cooling and solidification [13]. The physical mixture was used as a control and the samples were characterized using Thermogravimetry (TG/DTG), Differential Scanning Calorimetry (DSC), Fourier transform infrared spectroscopy (FTIR) and Polarized Light Microscopy (PLM) [16,17].

2.2.2. Solid lipid nanoparticles production and freeze-drying

SLN were produced using the high shear homogenization method described by Souto et al. [3], followed by lyophilization. The oil phase was composed of cetyl palmitate (0.10% m/V), soy lecithin (0.15% m/V), and ethanol 5 mL. The aqueous phase was composed of an aqueous solution of Tween®20 (0.10% m/V). Each phase undergone homogenization with magnetic stirring (KASVI, model K40–1820H, Brazil) for 5 min at ~85 °C. Subsequently, the lipid phase was dripped into the aqueous phase and homogenized in a high shear homogenization (Ultra-Turrax® T25, USA), at 8000 rpm for 10 min and 90 °C. The obtained SLN were cooled down to room temperature under continuous magnetic stirring. The same procedure was used for the loading of PZQ into the lipid phase.

2.3. Characterization

2.3.1. Particle size measurement, polydispersity index, and zeta potential

SLN average size, polydispersity index, and zeta potential were determined by photon correlation spectroscopy (Malvern Zeta sizer, Nano Z-S; Malvern Instruments, Worcestershire, United Kingdom). Measurement settings used a 90° angle, 25 °C temperature, and a 633 mW He–Ne laser with a 632.8 nm wavenumber. All measurements were done in triplicate using diluted aliquots (1:100).

2.3.2. Encapsulation efficiency (EE)

EE was determined according to Kolenyak-Santos et al. [17]. To calculate EE%, 1 g of each PZQ-loaded SLN was dissolved in 5 mL of ethanol. The solutions were then ultra-centrifuged for 40 min at 4 to 16,000 rpm (Biofuge Strato, Hong Kong). After ultracentrifugation, a volume of 2 mL of the supernatant was collected and analysed by ultraviolet (UV) spectrophotometry with detection adjusted to 264 nm. EE% was calculated in triplicate using Equation (1).

$$EE\ (\%) = \frac{PZQ\ extracted\ from\ SLN}{teorical\ PZQ\ added}\ x\ 100 \quad (1)$$

2.3.3. Thermal analysis

Thermogravimetric analysis (TG) was performed in a TA Instruments (DTG-60, Shimadzu, Japan). Samples were subjected to thermal analysis, under a nitrogen atmosphere (N_2), in a temperature range from 25 to 600 °C, with a 50 mL/min gas flow rate and a 10 °C/min heating rate. Differential Scanning Calorimetry (DSC) was run in a DSC 2010 (TA Instruments, EUA) from 0 to 250 °C, under a nitrogen atmosphere (N_2), with a 50 mL/min gas flow rate and 10 °C/min heating ratio. About 6.0–8.0 mg of sample was accurately weighted in aluminium recipients [1,2].

2.3.4. Fourier transform infrared spectroscopy (FTIR)

About 1 mg of sample was mixed with 200 mg of potassium bromide (KBr) using an agate crucible until the mixture became a fine, homogeneous powder. The mixture was oven-dried (60 °C for 20 min) for residual moisture removal. The sample was then placed in a holder and subjected to the hydraulic press for tablet formation. The FTIR spectra were then recorded over a range of 450–4000 cm^{-1} with a resolution of 4 cm^{-1} for 32 scans for each sample in a IR Prestige 21 (Shimadzu, Japan).

2.3.5. Polarized light microscopy (PLM)

The samples were examined under a PLM (Olympus model BX-51 microscope), linked to a digital camera (LC Color Evolution, PL-A662). The images were scanned using the PixeLINK. The samples were heated above the melting point and placed between two glass plates. They were then observed in a polarized light microscope at room temperature (25 °C). All samples were analysed using 5–20× magnification.

2.3.6. Scanning electron microscopy (SEM)

The morphology of the produced SLN were checked by SEM (Hitachi TM 3000, Japan) operated at 05 kV. The samples were placed on carbon and subjected to vacuum tapes. The images were digitized and randomly captured.

2.3.7. In vitro release studies

The release profile of PZQ from PZQ-loaded SLN was assessed against using the dialysis method. Prior to the assay, the dialysis bags (dialysis cellulose membrane, Sigma Aldrich, 25 mm) were kept in a phosphate buffer solution at room temperature for 24 h to remove the preservative, and then the bags were boiled in distilled water for 1 h. Approximately 2 mL of samples were placed in the pre-treated dialysis bag of 5 cm initial length and 25 mm flat width. The final length of the bag after the lashing was 5 ± 0.2 cm. The dialysis bags were then placed in a 50 mL beaker containing 10 mL of water and 40 mL phosphate buffer solution, pH 7.0 ± 0.4 and submerged. To simulate the *in vivo* conditions, the temperature and the rotational speed were set at 37 ± 0.5 °C and 100 rpm, respectively. At pre-determined time

intervals (0, 5, 10, 15, 30, 60, 120 and 180 min), a volume of 200 μL of the release medium was collected, filtered through membrane pores of 0.45 μm and analysed in UV spectrophotometer (UV-VIS Spectrophotometer, Model UV2600 Shimadzu, Japan). The same volume of fresh phosphate buffer solution at the same temperature was added immediately to keep the release volume constant.

2.4. Biological analysis

2.4.1. Cell viability in L929 cells in vitro

For the cell viability testing, the Methyl-thiazolyl-tetrazolium (MTT) colorimetric assay was carried out in a human fibroblast cell line (L929) and following the ISO 10993-5 (2009). SLN were used in a concentration of 30 μg/mL. L929 cells were seeded in 96-well culture plates (2 x 10^4 cells/well). A solution of MTT (0.5 mg/mL) was placed in contact with the cells, which were then incubated at 37 °C for 3 h. After removal of the MTT, dimethyl sulfoxide (150 μL) was placed for tetrazole salt crystals solubilization, and optical density reading was performed in an automated plate reader in a 570 nm wavelength. The tests were conducted in quadruplicate and then normalized [18].

2.4.2. In vitro treatment

Adult *Schistosoma mansoni* parasites (BH strain) were recovered from Swiss mice [19]. Mice were euthanized, and parasites were retrieved from portal system and mesenteric veins, washed in saline solution and then washed in RPMI-1640 medium. 24-well culture plates were prepared with 2 ml of RPMI-1640 medium (as a control group), and a couple of worms was added per well. PZQ and PZQ-loaded SLN and drug-free SLN were solubilized (0.25 μg/ml; 0.5 μg/ml; 1 μg/ml; 1.5 μg/ml) in PBS buffer and added to the culture plates. The parasites were incubated in an oven at 37 °C under a 5% CO_2 atmosphere and held for 72 h. Plaques were observed at 2, 4, 6, 12, 24, 48 and 72 h. The observed, classified and recorded parameters were the mobility, contraction, tegument damage and parasite death. Each formulation was evaluated in three wells per plate, and three replicates were performed for each of these. In all plates, three couples were used as a negative control [18].

2.4.3. Statistical analysis

The data obtained were expressed as the mean ± standard error of the mean (S.E.M.) and the differences between the experimental groups were evaluated using one-way ANOVA followed by the Tukey post-test. Significant values were set as $p < 0.05$. All statistical analyses were performed using the GraphPad Prism (Intuitive Software for Science, San Diego, CA, USA).

3. Results and discussion

3.1. Pre-formulation studies

Fig. 1 shows the PLM pictures of cetyl palmitate and its binary mixtures with PZQ before (A) and after (B) thermal treatment. All the samples were anisotropic with birefringent points. It is known that thermal stress as that induced by the heating above the melting point promotes changes in the microstructure of lipid materials [14,15]. Before the lipid mixture reaches the melting temperature, all samples exhibited needle-like structures, with reduced size and width with the increasing concentrations of PZQ. A similar result was described by Galvão et al. [20] suggesting that size and thickness reduction in lipid microstructures are linked to the decrease of the lipid crystallinity.

For the confirmation of the polymorphic changes and crystallinity of the lipids before and after the production of SLN [14], TG/DTG and DSC have been carried out (Figs. 2–4).

Fig. 2 shows the TG/DTG curves of the physical mixtures of cetyl palmitate and PZQ in different ratios before (A) and after (B) heating the samples above the melting point of the lipid. All samples exhibited a

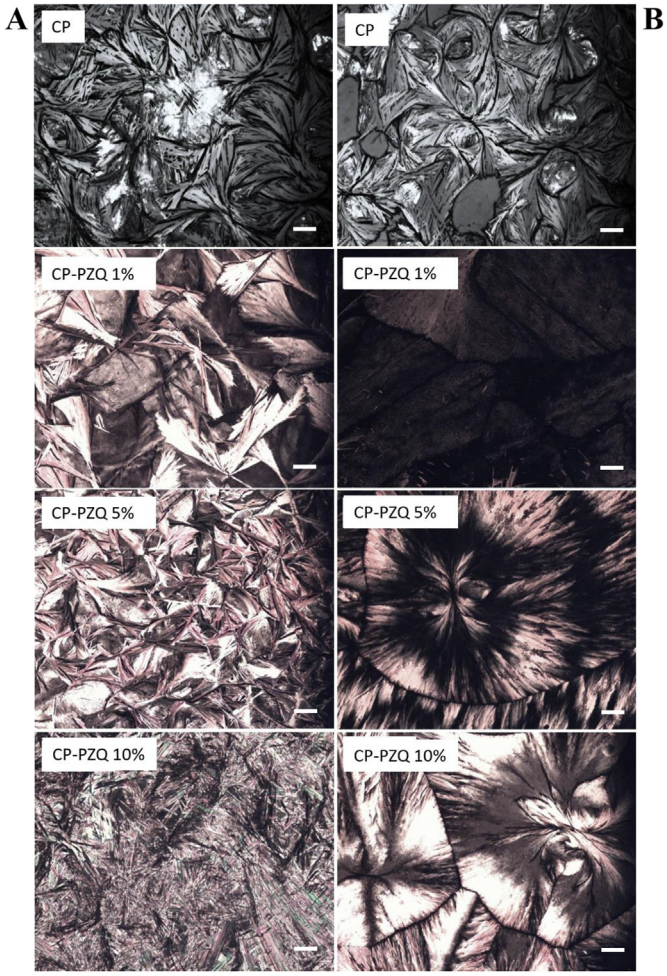

Fig. 1. PLM pictures taken before (A) and after (B) heating the samples (cetyl palmitate (CP) and binary mixtures containing 1% (CP-PZQ 1%), 5% (CP-PZQ 5%) and 10% (CP-PZQ 10%) of praziquantel) above the melting point of the lipid. Images obtained using 10× magnification, bar 100 μm.

single mass loss event between 200 and 350 °C. Fig. 2 (B) illustrates the TG/DTG curves of the binary mixtures after treatment. The mass losses found were Δm = 83% for 1%; 99% for 5% and 96% for 10% PZQ, with the respective DTG peaks at 346, 336 and 347 °C. When comparing the mass losses with those of untreated samples (Fig. 2 (A)), the values remained close (Δm ~ 96% for all samples), also recorded as single events between 204 °C and 344 °C (DTG_{peak} = 335, 340 and 348 °C for 1%, 5% and 10% PZQ, respectively). Such losses are characteristic of the presence of lipids.

From the obtained results, 1% cetyl palmitate-PZQ (CP-PZQ) mixture was selected for further studies due to the lower crystallinity which is associated with a higher loading capacity of the lipid for the drug. Fig. 3 shows the DSC curves of PZQ (a), CP-PZQ with heating (b), CP-PZQ without heating (c), CP with heating (d) and CP without heating (e).

Fig. 3 (a) shows an endothermic event at 144 °C for the free PZQ, which has also been reported in previous works [4,19,21]. The bulk lipid cetyl palmitate (CP) showed its endothermic events at 56.74 °C after (b) and at 57.24 °C before (c) thermal treatment. The change in the melting temperature was minimal but with a significant decrease of the enthalpy with the heating. Triglycerides are known to exhibit three main polymorphic forms (α, β'- and β) [22], and the shown variation in the enthalpy may correspond to the change from the amorphous α-form to the most stable β-modification [23].

The use of binary mixtures in thermal characterizations provides

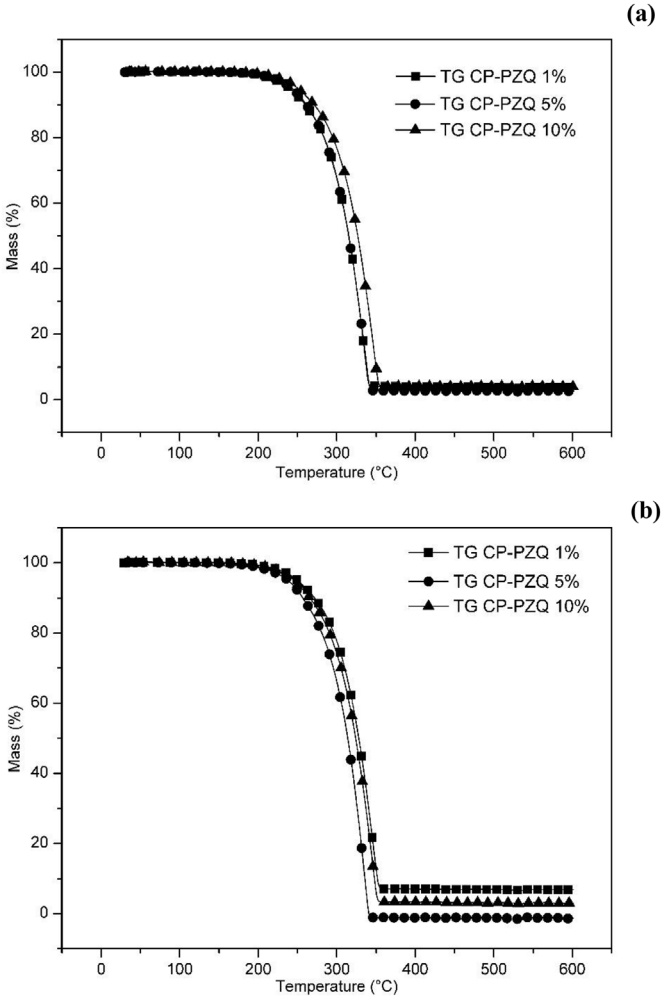

Fig. 2. TG/DTG curves of the physical mixtures of cetyl palmitate and praziquantel in different proportions before (A) and after (B) heating the samples above the melting point of the lipid.

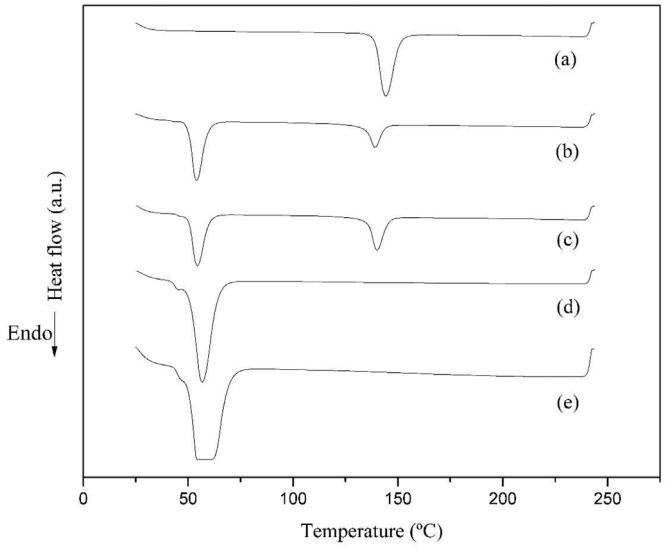

Fig. 3. DSC curves of (a) PZQ; (b) CP-PZQ 1% with heating; (c) CP-PZQ 1% without heating; (d) CP with heating and (e) CP without heating.

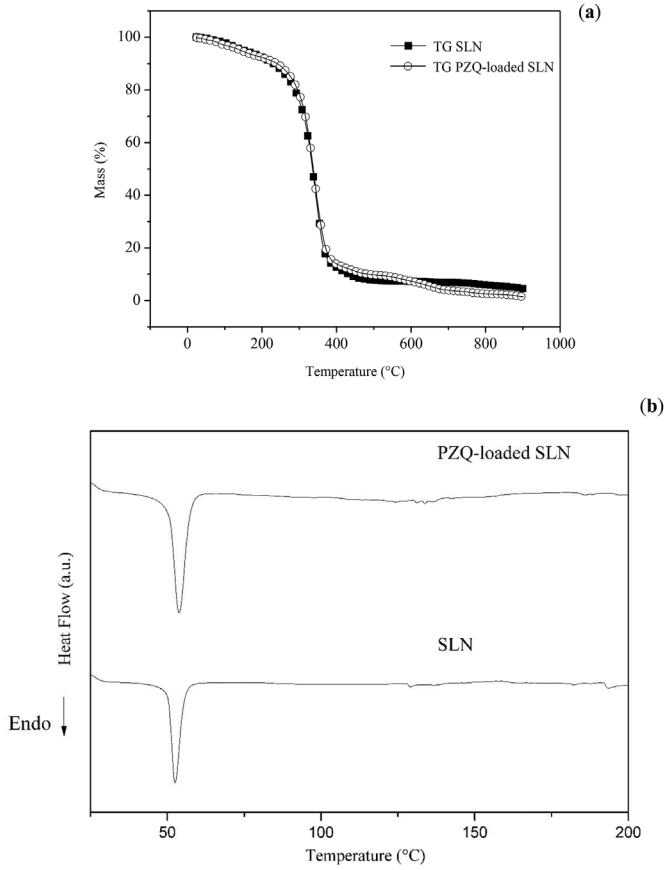

Fig. 4. (a) TG and (b) DSC curves for blank SLN and PZQ-loaded SLN.

information regarding the solubility and eventual interactions between drug and lipid matrix of SLN [24]. Analysing the CP-PZQ 1% before and after the thermal stress showed the typical melting peak of the bulk cetyl palmitate from 53.90 °C (before heating) and 54.84 °C (after heating). The presence of PZQ reduced and shifted to lower temperature values (T_{peak} 139.30 and 140.11 °C, respectively), attributed to the partial solubility of PZQ in the lipid matrix and interaction between these materials. Interactions observed by the DSC do not necessarily mean incompatibilities, but a structure reorganization [24].

3.2. SLN characterization

Blank SLN and PZQ-loaded SLN were evaluated for size, polydispersity index and zeta potential using photon correlation spectroscopy. The results are shown in Table 1. The mean particle size of blank SLN and PZQ-loaded SLN were 313.80 ± 0.44 and 324.40 ± 8.15, respectively. The highest values were obtained when loading the particles with the drug. The PI of blank SLN and PZQ-loaded SLN were

Table 1
R^2 values different mathematical fitting models for the release profile of PZQ and PZQ-loaded SLN.

Mathematical models	Square R value (R^2)	
	PZQ	PZQ-loaded SLN
Baker and Lonsdale	−0.4559	**0.8894**
Peppas	**0.8215**	**1.0**
Hixon and Crowell	−2.2413	**0.9999**
Higuchi, Square Root	−0.4665	**0.9035**
First Order	−2.2292	**0.9999**
Weibull 5 parameters	**1.0**	0.538

0.26 ± 0.007 nm and 0.24 ± 0.012 nm, respectively, showing a homogeneous size distribution i.e. below 0.5, which is appropriate for oral administration. The lower the polydispersity index values the lower the risk of particle aggregation attributed to a more homogeneous size distribution [25]; a higher PI is however always expected for SLN produced by high shear homogenization [4].

Zeta potential was determine also to predict physicochemical stability measuring electric charge at nanoparticle surface [26]. A higher zeta potential is always desirable in nanoparticle formulations [27]. Values for blank SLN and PZQ-loaded SLN were −29.27 ± 0.76 mV and −27.25 ± 0.59 mV, respectively. All samples exhibited negative zeta potential attributed to the presence of soybean lecithin, a surfactant capable of stabilizing the pre-emulsion by forming a protective layer around the oil droplets obtained from melted lipid, reducing surface tension and avoiding particle aggregation [28].

The EE of PZQ in cetyl palmitate nanoparticles reached 92.3%, which was higher than previous reports. Misha et al. produced PZQ-loaded SLN with a EE of 86.6 ± 5.72% to improve the oral bioavailability of PZQ by targeting the intestinal lymphatic system [2].

TG curves shown in Fig. 4 (a) exhibit a single-phase thermal decomposition for all samples in the temperature range between 200 °C and 300 °C. These findings suggest that formulations and their components remain stable throughout pre-formulation studies. Also, final residual mass of blank SLN was 8%, and of PZQ-loaded SLN was 2%.

Blank SLN and PZQ-loaded SLN DSC curves, enthalpy and melting temperature are depicted in Fig. 4 (b). PZQ-loaded SLN exhibited an endothermic peak at 54 °C (ΔH = −65.82 J/g. The loading of PZQ in SLN is suggested by the absence of the corresponding (endothermic) melting event peak of PZQ at 144 °C. The calorimetric curves of blank SLN exhibited one endothermic event at T_{peak} 52.64 °C (T_{onset} 49.41 °C), below the melting point of bulk cetyl palmitate. T_{peak} decreases suggests the rearrangement of lipid molecules within nanoparticles in a more unorganized pathway [29]. PZQ-loaded SLN showed a T_{peak} endothermic event at approximately 53.82 °C (T_{onset} 49.89 °C), confirming that no relevant modification in the crystalline structure occurred in the loaded SLN in comparison to the non-loaded particles. Non-encapsulated PZQ did not significantly change the melting temperature; however, the enthalpy of SLN increased from −83.85 J/g to −65.85 J/g) upon the loading of PZQ. This result is attributed to the energy needed to break cohesive force [30], supporting the PZQ encapsulation in cetyl palmitate SLN.

FTIR allows the identification of materials functional groups. Fig. 5 depicts the FTIR spectra of cetyl palmitate, PZQ, blank SLN, PZQ-loaded SLN, and soybean lecithin. The PZQ sample showed as carbonyl stretch vibrations –C = O (1630 cm^{-1}), –CH, $–CH_2$, $–CH_3$ (2900-3000 cm^{-1}), CN stretch vibrations (1000-1350 cm^{-1}). Soybean lecithin samples exhibited broad peaks at –CH, $–CH_2$, $–CH_3$ elongation (2850-3000 cm^{-1}), carbonyl stretch vibrations - C = O (1700-1800 cm^{-1}), stretching of CO (1050 - 1250 cm^{-1}) and OH-stretching vibrations (3200 - 3500 cm^{-1}). Cetyl palmitate exhibited peaks at 2921, 2850 and 1464 cm^{-1} assigned to methyl type C–H bonds, in addition to one at 1734 cm^{-1} attributed to C = O bonds in ester groups derived from carboxylic acids., These results confirm previously published works from other groups [31]). Absorption peaks can be observed throughout the different sample. The difference between blank SLN and PZQ-loaded SLN spectra is remarkable. However, both samples share bands characteristic of methylene groups CH bonds (2921, 2850 and 17467 cm^{-1}), C = O ester group vibrations at 1737 cm^{-1}, which are linked to their composition in cetyl palmitate and in soy lecithin. Only the blank SLN exhibited ester-like vibrations at 1085 cm^{-1} for lecithin.

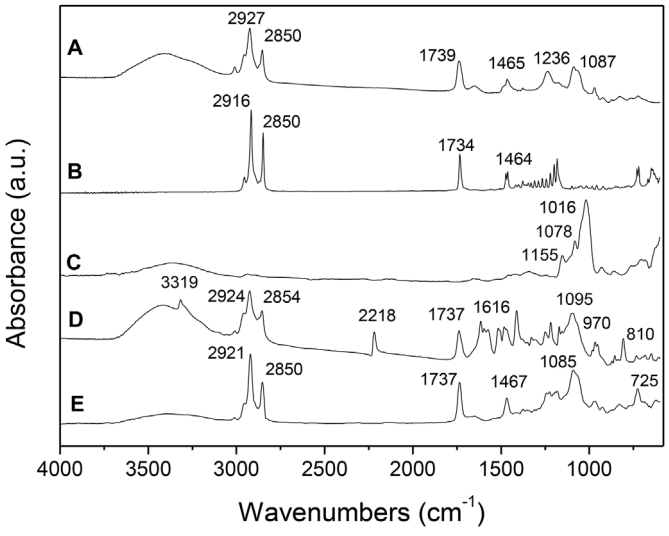

Fig. 5. Infrared spectra of (A) soybean lecithin, (B) cetyl palmitate, (C) PZQ, (D) PZQ-loaded SLN, and (E) blank SLN.

The presence of PZQ in the formulation induced changes in the spectrum profile of SLN with additional peaks within 3423-3300 cm^{-1}, attributed to primary amines and alcohols, respectively, of lecithin and PZQ; the stretch of C = C of the aromatic ring at 1616 cm^{-1}; and the C–N bond in 2218 cm^{-1}. These data corroborate the work of Kolenyak-Santos et al. [17]. Peak changes are an indication of interactions in the system, again suggesting that PZQ was indeed loaded within lipid matrices of SLN.

Fig. 6 shows the SEM images of PZQ-loaded SLN at three different resolutions to analyse their morphology. PZQ-loaded SLN were typically spherical with sizes between 500 and 1000 nm. Sample agglomeration was due to evaporation during lyophilization process and is caused by London-van der Waals forces becoming dominant to the repulsion. Thus, surfactants are an alternative during the synthesis process to avoid SLN agglomeration.

3.3. In vitro release studies

PZQ release profile was evaluated after determining the drug concentration in the dissolution medium and the results are expressed as a percentage of drug released versus time (Fig. 7). The release occurred in a controlled manner, and after 60 min, less than 10% of all incorporated PZQ had been released.

PZQ-loaded SLN formulations followed a slow release profile, without promoting a considerable PZQ increase in the medium within a period of 1 h. Drug release from SLN can be affected by several factors, e.g. the particle size and porosity, shape, drug physical state and molar mass, production parameters, type of surfactant and its concentration, the polymorphism of the lipid matrix, drug solubility and drug partition coefficient in the lipid matrix, drug diffusion distance in the lipid matrix, among others [23,32,33].

The loading of drugs in SLN is a recognised strategy to improve the solubility profile of poorly water-soluble drugs [34]. According to Passerini et al. [35], who formulated PZQ in Gelucire 50/13 microspheres, different mechanisms can increase drug dissolution in aqueous medium, e.g. by improving the wetting degree of the nanoparticles by increasing their hydrophilic character, by particle size reduction, or by using an amorphous form of the drug compound. Drug change from a crystalline structure to an amorphous state should be a factor to be considered, since the amorphous forms are more soluble than the crystalline ones, having a higher dissolution rate [33].

The increase of the particle size is associated with the reduction of the release rate because the drug has to overcome more lipid per particle to reach the release medium [36]. The diffusion coefficient of the drug through the lipid matrix may also be attributed to eventual drug-lipid interactions. The amount of lipid used may also contribute to the delay in release. According to Souto et al. [37], a higher lipid percentage generates a lower diffusion rate, as the drug core is covered by a lipid shell than controls the release from the particles. On the other

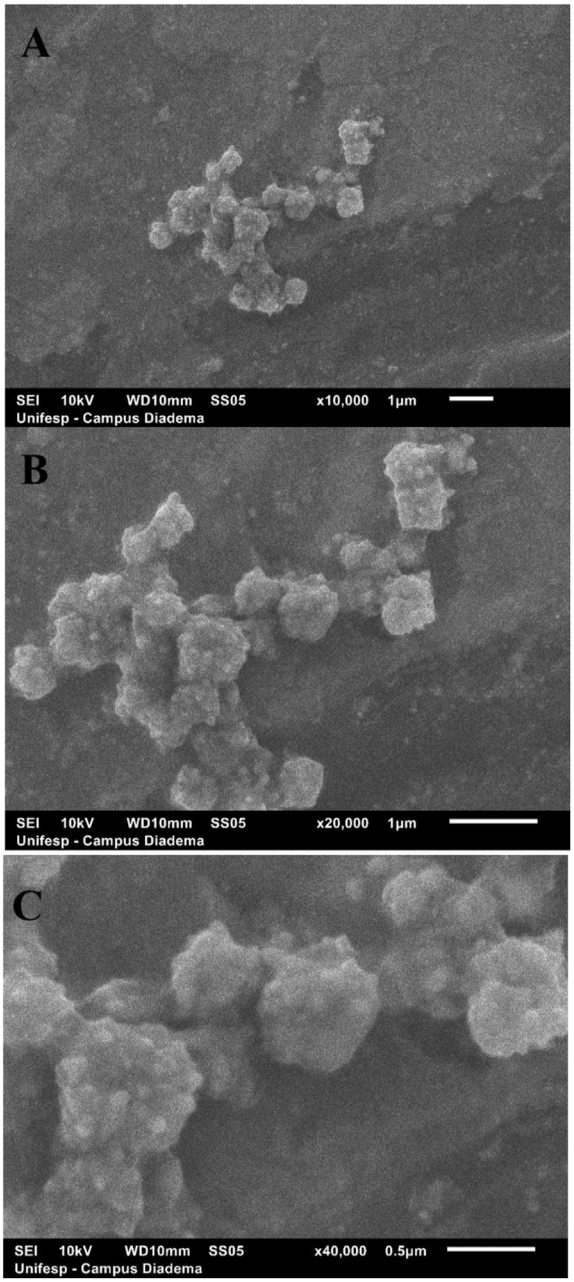

Fig. 6. Scanning electron photomicrographs of PZQ-loaded SLN (a) x 10000, (b) x 20000, (c) x 40000.

hand, lower lipid concentrations produce a drug-enriched shell model where the drug is placed on the surface of the nanoparticle showing less capacity for controlled release. Upon cooling-down the freshly prepared SLN, lipid recrystallization from the liquid to solid state occurs, the drug reduces its partitioning in water and is retained by the lipid during the generation of solid lipid matrices of SLN. This mechanism causes drug retention within nanoparticles, slowing down its release profile [38,39].

The release mechanism was determined by calculating the R^2 value for each selected kinetic model i.e. Baker and Lonsdale, Peppas, Hixon and Crowell, Higuchi, Square Root, First Order, Weibull (Table 1). Peppas, Hixon, and Crowell (R^2 = 1.0) and First Order (R^2 = 0.99) exhibited the best fit for the produced PZQ-loaded SLN.

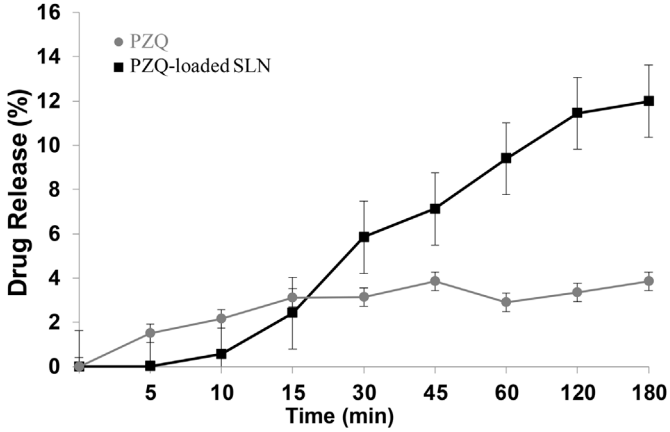

Fig. 7. *In vitro* drug release profile of free PZQ and SLN-PZQ.

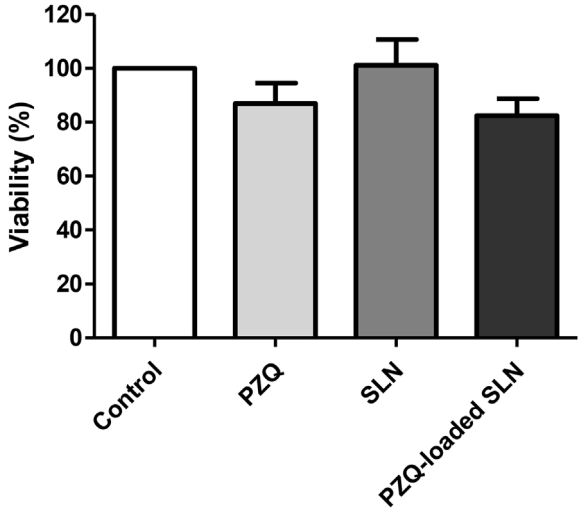

Fig. 8. Effect of praziquantel, blank SLN and PZQ-loaded SLN on the viability assessment of human L929 fibroblasts determined by MTT assay after 24 h of incubation. The negative control (C) was treated with the vehicle used to dilute the drug (DMSO 5%). The data correspond to the mean ± SD of four independent experiments.

3.4. *In vitro* assay

3.4.1. *Cell viability in L929 cell lines*

In vitro cytotoxicity assay was performed in human fibroblasts L929 as a cell model. The data are shown as cell viability percentage (Fig. 8). Cell viability results show that PZQ did not kill normal human fibroblasts; cellular viability was higher than 88%. Moreover, free PZQ and PZQ-loaded SLN also did not show toxicological activity. The results translate the safety and biocompatibility of free PZQ and PZQ-loaded SLN in fibroblasts cells.

According to Kolenyak-Santos et al. [5] and Salehzadeh et al. [6], the cytotoxic effects of the particles are linked to the cell membrane adhesion, particle internalization and product degradation within cell culture medium or inside cells. However, different cell types have different susceptibility to different types of nanoparticles. SLN are produced from natural lipids, thus they should be well-tolerated by living organisms [4,5]. In the cell viability assay against human fibroblasts (L2929), PZQ-loaded SLN showed 82.4% of viable cells, whilst blank SLN had 101.1% and isolated PZQ 86.9% of viable cells. There was no statistical significance ($p > 0.05$) between isolated PZQ and PZQ-loaded SLN. Thus, these formulations exhibit a safe profile for normal human cell lines, with anticipated no toxicological profile to the human organism.

Table 2
In vitro effect of PZQ, blank SLN and PZQ-loaded SLN on adult worms of *S. mansoni*. Evaluation was performed at several time points along an incubation period of 72 h. Median contraction and damage in the tegument of *S. mansoni* males: 0 – Absence of contraction/damage; 1 – Little contraction/damage; 2 – Moderate contraction/damage; 3 – High contraction/damage and rate mortality (%).

FORMULATION	CONCENTRATION	CONTRACTION MALES						
		2h	4h	6h	12h	24h	48h	72h
Blank SLN	0.25 μg/mL	3	3	3	3	3	3	3
	0.5 μg/mL	3	3	3	3	3	3	3
	1.0 μg/mL	3	3	3	3	3	3	3
	1.5 μg/mL	3	3	3	3	3	3	3
	2 μg/mL	3	3	3	3	3	3	3
	4 μg/mL	3	3	3	3	3	3	3
	8 μg/mL	3	3	3	3	3	3	3
	10 μg/mL	3	3	3	3	3	3	3
	0 μg/mL	3	3	3	3	3	3	3
PZQ-loaded SLN	0.25 μg/mL	3	3	3	2	2	2	2
	0.5 μg/mL	2	2	2	2	2	2	2
	1.0 μg/mL	2	2	1	1	1	1	1
	1.5 μg/mL	1	1	1	1	1	1	1
	2 μg/mL	1	1	1	1	1	1	1
	4 μg/mL	1	1	1	1	1	0	0
	8 μg/mL	1	1	0	0	0	0	0
	10 μg/mL	0	0	0	0	0	0	0
	0 μg/mL	3	3	3	2	2	2	2
PZQ	0.25 μg/ml	3	3	3	3	3	3	3
	0.5 μg/ml	2	1	1	1	1	1	1
	1 μg/ml	1	1	1	1	1	1	1
	1.5 μg/ml	1	1	1	1	1	1	1
	0 μg/mL	1	1	0	0	0	0	0
FORMULATION	**CONCENTRATION**	**TEGUMENTARY DAMAGE**						
		2h	**4h**	**6h**	**2h**	**24h**	**48h**	**72h**
Blank SLN	0.25 μg/mL	0	0	0	0	0	0	0
	0.5 μg/mL	0	0	0	0	0	0	0
	1.0 μg/mL	0	0	0	0	0	0	0
	1.5 μg/mL	0	0	0	0	0	0	0
	2 μg/mL	0	0	0	0	0	0	0
	4 μg/mL	0	0	0	0	0	0	0
	8 μg/mL	0	0	0	0	0	0	0
	10 μg/mL	0	0	0	0	0	0	0
	0 μg/mL	0	0	0	0	0	0	0
PZQ-loaded SLN	0.25 μg/mL	0	0	0	1	1	1	1
	0.5 μg/mL	1	1	1	1	1	1	1
	1.0 μg/mL	2	2	2	3	2	2	2
	1.5 μg/mL	2	2	2	3	3	3	3
	2 μg/mL	2	3	3	3	3	3	3
	4 μg/mL	2	3	3	3	3	3	3
	8 μg/mL	2	3	3	3	3	3	3
	10 μg/mL	2	3	3	3	3	3	3
	0 μg/mL	1	2	3	3	3	3	3
PZQ	0.25 μg/ml	1	1	2	2	3	3	3
	0.5 μg/ml	2	2	3	3	3	3	3
	1.0 μg/ml	2	3	3	3	3	3	3
	1.5 μg/ml	2	3	3	3	3	3	3
	0 μg/ml	0	0	0	0	0	0	0
FORMULATION	**CONCENTRATION**	**MORTALITY (%)**						
		2h	**4h**	**6h**	**2h**	**24h**	**48h**	**72h**
Blank SLN	0.25 μg/mL	0	0	0	0	0	0	0
	0.5 μg/mL	0	0	0	0	0	0	0
	1.0 μg/mL	0	0	0	0	0	0	0
	1.5 μg/mL	0	0	0	0	0	0	0
	2 μg/mL	0	0	0	0	0	0	0
	4 μg/mL	0	0	0	0	0	0	0
	8 μg/mL	0	0	0	0	0	0	0
	10 μg/mL	0	0	0	0	0	0	0
	0 μg/mL	0	0	0	0	0	0	0

(*continued on next page*)

Table 2 (*continued*)

FORMULATION	CONCENTRATION	CONTRACTION MALES						
		2h	4h	6h	12h	24h	48h	72h
PZQ-loaded SLN	0.25 μg/mL	0	0	0	0	0	0	0
	0.5 μg/mL	0	0	0	0	0	0	0
	1.0 μg/mL	0	0	0	0	0	0	0
	1.5 μg/mL	0	0	0	0	0	0	0
	2 μg/mL	0	0	0	0	0	0	0
	4 μg/mL	0	0	33	33	33	89	89
	8 μg/mL	11	11	67	67	89	100	100
	10 μg/mL	100	100	100	100	100	100	100
	0 μg/mL	0	0	0	0	0	0	0
PZQ	0.25 μg/ml	0	0	0	0	0	0	0
	0.5 μg/ml	0	0	0	0	0	0	0
	1.0 μg/ml	0	0	0	0	22	22	56
	1.5 μg/ml	11	11	11	78	100	100	100
	0 μg/ml	0	0	0	0	0	0	0

3.4.2. In vitro effect of PZQ, blank SLN and PZQ-loaded SLN on contractility and tegumentary damage of female and male worms of S. mansoni

For the assessment of the *in vitro* effect of PZQ, blank SLN and PZQ-loaded SLN on the contractility and tegumentary damage of *S. mansoni*, adult *S. mansoni* worms were placed in RPMI-1640 medium (control group) and exposed to the formulations (0.25–10 μg/ml in PBS). When compared to the control group (RPMI-1640), the effect of free PZQ on *S. mansoni* culture was significant, as it caused changes in the integument and contraction of female and male worms evaluated at concentrations of 0.25–10 μg/ml. The effect on the mean contraction for male worms exposed to PZQ (0.25 μg/ml) was moderate after 6 h of exposure. PZQ (0.5 μg/ml) exhibited maximum contraction after 12 h of exposure, and the same occurred for PZQ (1.5 μg/ml) (Table 2).

According to Cupit and Cunningham [40], although PZQ has been the leading treatment for schistosomiasis for many years, its precise mechanism of action remains unknown. When helminths come into contact with PZQ *in vitro*, they immediately suffer a rapid influx of Ca^{2+} followed by intense muscle paralysis. Another notable feature is vacuolization and damage in the integument and subtegumentary structures in adults, but not in young forms [41]. This impair the integument and expose parasite surface antigens leading to recognition and parasite clearance by host immune system, which may indirectly explain the difference in sensitivity between the younger and mature stages.

The treatment with PZQ also modulates different molecular pathways activation for *S. mansoni* female and male worms, which may be linked to sex-specific resistances [32]. Females are more susceptible to contraction than males, and both PZQ and PZQ-loaded SLN exhibited a considerable contraction in the concentration of 1 μg/ml after 2 h of exposure.

PZQ (0.25 μg/ml) presented maximum worm integument damage after 24 h of drug exposure. For PZQ (0.5 μg/ml), moderate damage to the integument was observed in the first 2–4 h of exposure, and maximum damage after 6 h of exposure. The same results were found for higher concentrations 1 and 1.5 μg/ml.

PZQ-loaded SLN (1.5 μg/ml) exhibited maximum worm integument damage after 12 h of exposure. It was observed that female worms tegumentary damage profiles exposed to PZQ-loaded SLN were less intense when compared with *S. mansoni* male worms. PZQ-loaded SLN (0.25 μg/ml) exhibited maximum worm integument damage at the lowest concentration after 24 h of exposure. For the other concentrations, maximum damage was reached within the first 2 h of exposure.

PZQ-loaded SLN (4 μg/ml) caused 33% death percentage 6 h after exposure, and 89% male worm mortality after 48 h. PZQ-loaded SLN (8 μg/ml) caused 100% parasite death after 48 h. Females proved to be more resistant and needed concentrations of 10 μg/ml and 48 h to reach 100% parasite death. It is noteworthy that for the isolated PZQ only 56% of female worms died and PZQ alone did not reach 100% female parasite death. Thus, PZQ-loaded SLN to effectively reach parasite membrane contributes to parasite destruction (Table 3).

These results indicate that PZQ-loaded SLN should be capable of inducing parasite death more efficiently than conventional PZQ treatment. Appropriate SLN modification, and the fact that they are made from physiological compounds, overcome several biological barriers, being effectively delivered to the target site, which minimizes the risk of chronic toxicity [42,43]. Also, adequate SLN surface modification can significantly reduce the initial burst release of the encapsulated drug [44].

4. Conclusions

We demonstrate that PZQ-loaded SLN provides higher schistosomicidal activity against a *S. mansoni* culture when compared to the regular PZQ treatment. PZQ-loaded SLN can improve drug solubility with no signs of toxicity in human fibroblast cell cultures. Therefore, SLN can be used to produce liquid and solid formulations for schistosomiasis control, specially in endemic regions, improving therapeutic efficacy and reducing the PZQ toxic effects.

CRediT authorship contribution statement

Luciana Nalone Andrade: Formal analysis, Visualization, Writing - original draft, Conceptualization, Methodology, Formal analysis, Investigation, Resources, Data curation. **Conrado Marques:** Formal analysis, Visualization, Writing - original draft, Conceptualization, Methodology, Formal analysis, Investigation, Resources, Data curation. **Thallysson Barbosa:** Formal analysis, Visualization, Writing - original draft, Conceptualization, Methodology, Formal analysis, Investigation, Resources, Data curation. **Rafael Santos:** Formal analysis, Visualization, Writing - original draft, Conceptualization, Methodology, Formal analysis, Investigation, Resources, Data curation. **Marco Vinícius Chaud:** Writing - original draft, Conceptualization, Methodology, Formal analysis, Investigation, Resources, Data curation. **Classius Ferreira da Silva:** Writing - original draft, Conceptualization, Methodology, Formal analysis, Investigation, Resources, Data curation. **Cristiane Bani Corrêa:** Writing - original draft, Conceptualization, Methodology, Formal analysis, Investigation, Resources, Data curation. **Ricardo Guimaraes Amaral:** Writing - original draft, Conceptualization, Methodology, Formal analysis, Investigation, Resources, Data curation. **Rogéria de Souza Nunes:** Writing - original draft, Conceptualization, Methodology, Formal analysis, Investigation, Resources, Data curation. **Joyce Kelly M.C. Gonsalves:** Writing -

Table 3
In vitro effect of PZQ, blank SLN e PZQ-loaded SLN on adult worms of *S. mansoni*. Evaluation was performed at several time points along an incubation period of 72 h. Median contraction and damage in the tegument of *S. mansoni* females: 0 – Absence of contraction/damage; 1 – Little contraction/damage; 2 – Moderate contraction/damage; 3 – High contraction/damage and rate mortality (%).

FORMULATION	CONCENTRATION	CONTRACTION FEMALES						
		2h	4h	6h	12h	24h	48h	72h
Blank SLN	0.25 μg/mL	0	0	0	0	0	0	0
	0.5 μg/mL	0	0	0	0	0	0	0
	1.0 μg/mL	0	0	0	0	0	0	0
	1.5 μg/mL	0	0	0	0	0	0	0
	2 μg/mL	0	0	0	0	0	0	0
	4 μg/mL	0	0	0	0	0	0	0
	8 μg/mL	0	0	0	0	0	0	0
	10 μg/mL	0	0	0	0	0	0	0
	0 μg/mL	0	0	0	0	0	0	0
PZQ-loaded SLN	0.25 μg/mL	0	0	0	0	0	0	0
	0.5 μg/mL	0	0	0	0	0	0	0
	1.0 μg/mL	1	1	1	1	1	1	1
	1.5 μg/mL	1	1	2	2	2	2	2
	2 μg/mL	1	1	2	2	2	2	2
	4 μg/mL	2	2	2	2	2	2	2
	8 μg/mL	2	2	3	3	3	3	3
	10 μg/mL	2	3	3	3	3	3	3
	0 μg/mL	0	0	0	0	0	0	0
PZQ	0.25 μg/ml	1	1	2	2	2	2	2
	0.5 μg/ml	2	3	3	3	3	3	3
	1 μg/ml	3	3	3	3	3	3	3
	1.5 μg/ml	3	3	3	3	3	3	3
	0 μg/mL	0	0	0	0	0	0	0
FORMULATION	**CONCENTRATION**	**TEGUMENTARY DAMAGE**						
		2h	**4h**	**6h**	**2h**	**24h**	**48h**	**72h**
Blank SLN	0.25 μg/mL	0	0	0	0	0	0	0
	0.5 μg/mL	0	0	0	0	0	0	0
	1.0 μg/mL	0	0	0	0	0	0	0
	1.5 μg/mL	0	0	0	0	0	0	0
	2 μg/mL	0	0	0	0	0	0	0
	4 μg/mL	0	0	0	0	0	0	0
	8 μg/mL	0	0	0	0	0	0	0
	10 μg/mL	0	0	0	0	0	0	0
	0 μg/mL	0	0	0	0	0	0	0
PZQ-loaded SLN	0.25 μg/mL	0	0	0	0	0	0	0
	0.5 μg/mL	0	0	0	0	0	0	0
	1.0 μg/mL	1	2	2	2	2	2	2
	1.5 μg/mL	2	2	2	2	2	2	2
	2 μg/mL	2	2	2	2	2	2	2
	4 μg/mL	2	3	3	3	3	3	3
	8 μg/mL	2	3	3	3	3	3	3
	10 μg/mL	2	3	3	3	3	3	3
	0 μg/mL	0	0	0	0	0	0	0
PZQ	0.25 μg/ml	1	1	1	2	2	3	3
	0.5 μg/ml	1	2	3	3	3	3	3
	1.0 μg/ml	2	2	3	3	3	3	3
	1.5 μg/ml	2	3	3	3	3	3	3
	0 μg/ml	0	0	0	0	0	0	0
FORMULATION	**CONCENTRATION**	**MORTALITY (%)**						
		2h	**4h**	**6h**	**2h**	**24h**	**48h**	**72h**

Table 3 (*continued*)

FORMULATION	CONCENTRATION	CONTRACTION FEMALES						
		2h	4h	6h	12h	24h	48h	72h
Blank SLN	0.25 μg/mL	0	0	0	0	0	0	0
	0.5 μg/mL	0	0	0	0	0	0	0
	1.0 μg/mL	0	0	0	0	0	0	0
	1.5 μg/mL	0	0	0	0	0	0	0
	2 μg/mL	0	0	0	0	0	0	0
	4 μg/mL	0	0	0	0	0	0	0
	8 μg/mL	0	0	0	0	0	0	0
	10 μg/mL	0	0	0	0	0	0	0
	0 μg/mL	0	0	0	0	0	0	0
PZQ-loaded SLN	0.25 μg/mL	0	0	0	0	0	0	0
	0.5 μg/mL	0	0	0	0	0	0	0
	1.0 μg/mL	0	0	0	0	0	0	0
	1.5 μg/mL	0	0	0	0	0	0	0
	2 μg/mL	0	0	0	0	0	0	0
	4 μg/mL	0	0	0	0	0	0	0
	8 μg/mL	0	0	0	0	44	56	67
	10 μg/mL	0	0	22	22	56	100	100
	0 μg/mL	0	0	0	0	0	0	0
PZQ	0.25 μg/ml	0	0	0	0	0	0	0
	0.5 μg/ml	0	0	0	0	0	0	0
	1.0 μg/ml	0	0	0	0	0	0	0
	1.5 μg/ml	0	0	11	44	44	56	56
	0 μg/ml	0	0	0	0	0	0	0

original draft, Conceptualization, Methodology, Formal analysis, Investigation, Resources, Data curation. **Silmara Allegretti:** Writing - original draft, Conceptualization, Methodology, Formal analysis, Investigation, Resources, Data curation. **Eliana B. Souto:** Project administration, Supervision, Funding acquisition, Writing - review & editing, Conceptualization, Methodology, Formal analysis, Investigation, Resources, Data curation. **Patrícia Severino:** Project administration, Supervision, Funding acquisition, Writing - review & editing, Conceptualization, Methodology, Formal analysis, Investigation, Resources, Data curation.

Declaration of competing interest

The authors report no conflict of interests with respect to this work.

Acknowledgments

The authors wish to acknowledge *Coordenação Aperfeiçoamento de Pessoal de Nivel Superior* (CAPES), *Fundação de Amparo à Pesquisa do Estado de Sergipe* (FAPITEC), Conselho Nacional de Desenvolvimento Científico e Tecnológico (CNPq, #443238/2014-6, #470388/2014-5). EBS wishes to acknowledge the financial support received from Portuguese Science and Technology Foundation (FCT/MCT) and from European Funds (PRODER/COMPETE) under the projects M-ERA-NET-0004/2015-PAIRED, co-financed by FEDER, under the Partnership Agreement PT2020.

Appendix A. Supplementary data

Supplementary data to this article can be found online at https://doi.org/10.1016/j.jddst.2020.101784.

References

[1] S. Pamu, T. Singh, J. Chandrudu, Schistosoma and Human Schistosomiasis, Educreation Publishing, 2018.
[2] D.H. Molyneux, L. Savioli, D. Engels, Neglected tropical diseases: progress towards addressing the chronic pandemic, Lancet 389 (2017) 312–325.
[3] V.B.R. da Silva, B.R.K.L. Campos, J.F. de Oliveira, J.-L. Decout, M.d.C.A. de Lima,

Medicinal chemistry of antischistosomal drugs: praziquantel and oxamniquine, Bioorg. Med. Chem. 25 (2017) 3259–3277.
[4] C.S.F. Marques, P. Rezende, L.N. Andrade, T.M.F. Mendes, S.M. Allegretti, C. Bani, M.V. Chaud, M. Batista-de-Almeida, E.B. Souto, L. Pereida-da-Costa, P. Severino, Solid dispersion of praziquantel enhanced solubility and improve the efficacy of the schistosomiasis treatment, J. Drug Deliv. Sci. Technol 45 (2018) 124–134.
[5] M. Malhado, D.P. Pinto, A.C. Silva, G.P. Silveira, H.M. Pereira, J.G. Santos Jr., C.V. Guilarducci-Ferraz, A.L. Viçosa, M. Nele, L.B. Fonseca, Preclinical pharmacokinetic evaluation of praziquantel loaded in poly (methyl methacrylate) nanoparticle using a HPLC–MS/MS, J. Pharmaceut. Biomed. Anal. 117 (2016) 405–412.
[6] L.D. Silva, E.C. Arrúa, D.A. Pereira, C.M. Fraga, T.L. da Costa, A. Hemphill, C.J. Salomon, M.C. Vinaud, Elucidating the influence of praziquantel nanosuspensions on the in vivo metabolism of Taenia crassiceps cysticerci, Acta Trop. 161 (2016) 100–105.
[7] F. Tomiotto-Pellissier, M.M. Miranda-Sapla, L.F. Machado, B.T. da Silva Bortoleti, C.S. Sahd, A.F. Chagas, J.P. Assolini, F.J. de Abreu Oliveira, W.R. Pavanelli, I. Conchon-Costa, Nanotechnology as a potential therapeutic alternative for schistosomiasis, Acta Trop. 174 (2017) 64–71.
[8] P. Severino, E.B. Souto, S.C. Pinho, M.H. Santana, Hydrophilic coating of mitotane-loaded lipid nanoparticles: preliminary studies for mucosal adhesion, Pharmaceut. Dev. Technol. 18 (2013) 577–581.
[9] A.L.R. de Souza, T. Andreani, R.N. De Oliveira, C.P. Kiill, F.K. dos Santos, S.M. Allegretti, M.V. Chaud, E.B. Souto, A.M. Silva, M.P.D. Gremião, In vitro evaluation of permeation, toxicity and effect of praziquantel-loaded solid lipid nanoparticles against Schistosoma mansoni as a strategy to improve efficacy of the schistosomiasis treatment, Int. J. Pharm. 463 (2014) 31–37.
[10] A. Mishra, P.R. Vuddanda, S. Singh, Intestinal lymphatic delivery of praziquantel by solid lipid nanoparticles: formulation design, in vitro and in vivo studies, J. Nanotechnol. (2014) 2014.
[11] S. Xie, B. Pan, M. Wang, L. Zhu, F. Wang, Z. Dong, X. Wang, W. Zhou, Formulation, characterization and pharmacokinetics of praziquantel-loaded hydrogenated castor oil solid lipid nanoparticles, Nanomedicine 5 (2010) 693–701.
[12] M.V. Chaud, P. Tamascia, A.C. de Lima, M.O. Paganelli, M.P.D. Gremião, O. de Freitas, Solid dispersions with hydrogenated castor oil increase solubility, dissolution rate and intestinal absorption of praziquantel, Braz. J. Pharmaceut . Sci. 46 (2010) 473–481.
[13] P. Severino, S.C. Pinho, E.B. Souto, M.H.A. Santana, Crystallinity of Dynasan® 114 and Dynasan® 118 matrices for the production of stable Miglyol®-loaded nanoparticles, J. Therm. Anal. Calorim. 108 (2011) 101–108.
[14] P. Severino, S.C. Pinho, E.B. Souto, M.H. Santana, Polymorphism, crystallinity and hydrophilic–lipophilic balance of stearic acid and stearic acid–capric/caprylic triglyceride matrices for production of stable nanoparticles, Colloids Surf. B Biointerfaces 86 (2011) 125–130.
[15] P. Severino, S.C. Pinho, E.B. Souto, M.H. Santana, Crystallinity of Dynasan® 114 and Dynasan® 118 matrices for the production of stable Miglyol®-loaded nanoparticles, J. Therm. Anal. Calorim. 108 (2011) 101–108.
[16] S. Doktorovova, R. Shegokar, L. Fernandes, P. Martins-Lopes, A.M. Silva, R.H. Muller, E.B. Souto, Trehalose is not a universal solution for solid lipid nanoparticles freeze-drying, Pharmaceut. Dev. Technol. 19 (2014) 922–929.
[17] F. Kolenyak-Santos, C. Garnero, R.N. De Oliveira, A.L. de Souza, M. Chorilli, S.M. Allegretti, M.R. Longhi, M.V. Chaud, M.P. Gremião, Nanostructured lipid carriers as a strategy to improve the in vitro schistosomiasis activity of praziquantel, J. Nanosci. Nanotechnol. 15 (2015) 761–772.
[18] N. Naseri, H. Valizadeh, P. Zakeri-Milani, Solid lipid nanoparticles and nanostructured lipid carriers: structure, preparation and application, Adv. Pharmaceut. Bull. 5 (2015) 305.
[19] A.L.R. de Souza, T. Andreani, F.M. Nunes, D.L. Cassimiro, A.E. de Almeida, C.A. Ribeiro, V.H.V. Sarmento, M.P.D. Gremião, A.M. Silva, E.B. Souto, Loading of praziquantel in the crystal lattice of solid lipid nanoparticles: studies by DSC and SAXS, J. Therm. Anal. Calorim. 108 (2011) 353–360.
[20] J.G. Galvao, G.G. Trindade, A.J. Santos, R.L. Santos, A.B. Chaves Filho, A.A.M. Lira, S. Miyamoto, R.S. Nunes, Effect of Ouratea sp. butter in the crystallinity of solid lipids used in nanostructured lipid carriers (NLCs), J. Therm. Anal. Calorim. 123 (2016) 941–948.
[21] M.V. Chaud, P. Tamascia, A.C.d. Lima, M.O. Paganelli, M.P.D. Gremião, O.d. Freitas, Solid dispersions with hydrogenated castor oil increase solubility, dissolution rate and intestinal absorption of praziquantel, Braz. J. Pharmaceut . Sci. 46 (2010) 473–481.
[22] V. Teeranachaideekul, E.B. Souto, V.B. Junyaprasert, R.H. Müller, Cetyl palmitate-based NLC for topical delivery of Coenzyme Q10–Development, physicochemical characterization and in vitro release studies, Eur. J. Pharm. Biopharm. 67 (2007) 141–148.
[23] T. Chantaburanan, V. Teeranachaideekul, D. Chantasart, A. Jintapattanakit, V.B. Junyaprasert, Effect of binary solid lipid matrix of wax and triglyceride on lipid crystallinity, drug-lipid interaction and drug release of ibuprofen-loaded solid lipid nanoparticles (SLN) for dermal delivery, J. Colloid Interface Sci. 504 (2017) 247–256.
[24] I.L. Dantas, K.T.S. Bastos, M. Machado, J.G. Galvão, A.D. Lima, J.K.M.C. Gonsalves, E.D.P. Almeida, A.A.S. Araújo, C.T. de Meneses, V.H.V. Sarmento, Influence of stearic acid and beeswax as solid lipid matrix of lipid nanoparticles containing tacrolimus, J. Therm. Anal. Calorim. 132 (2018) 1557–1566.
[25] A. Jain, K. Thakur, G. Sharma, P. Kush, U.K. Jain, Fabrication, characterization and cytotoxicity studies of ionically cross-linked docetaxel loaded chitosan nanoparticles, Carbohydr. Polym. 137 (2016) 65–74.
[26] V. Teeranachaideekul, T. Chantaburanan, V.B. Junyaprasert, Influence of state and crystallinity of lipid matrix on physicochemical properties and permeation of capsaicin-loaded lipid nanoparticles for topical delivery, J. Drug Deliv. Sci. Technol. 39 (2017) 300–307.
[27] S. Doktorovova, A.B. Kovacevic, M.L. Garcia, E.B. Souto, Preclinical safety of solid lipid nanoparticles and nanostructured lipid carriers: current evidence from in vitro and in vivo evaluation, Eur. J. Pharm. Biopharm. 108 (2016) 235–252.
[28] Y. Yamamoto, M. Araki, Effects of lecithin addition in oil or water phase on the stability of emulsions made with whey proteins, Biosc. Biotech. Biochem. 61 (1997) 1791–1795.
[29] E. Aboutaleb, F. Atyabi, M.R. Khoshayand, A.R. Vatanara, S.N. Ostad, F. Kobarfard, R. Dinarvand, Improved brain delivery of vincristine using dextran sulfate complex solid lipid nanoparticles: optimization and in vivo evaluation, J. Biomed. Mater. Res. 102 (2014) 2125–2136.
[30] A.A. Attama, S. Reichl, C.C. Müller-Goymann, Diclofenac sodium delivery to the eye: in vitro evaluation of novel solid lipid nanoparticle formulation using human cornea construct, Int. J. Pharm. 355 (2008) 307–313.
[31] K. Wang, Q.-j. Zhang, Y.-L. Miao, S.-Q. Luo, H.-C. Wang, W.-P. Zhang, Effect of solid lipid's structure on nanostructured lipid carriers encapsulated with sun filter: characterisation, photo-stability and in vitro release, J. Microencapsul. 34 (2017) 104–110.
[32] M.S. Ferreira, R.N. de Oliveira, D.N. de Oliveira, C.Z. Esteves, S.M. Allegretti, R.R. Catharino, Revealing praziquantel molecular targets using mass spectrometry imaging: an expeditious approach applied to Schistosoma mansoni, Int. J. Parasitol. 45 (2015) 385–391.
[33] L. Barthe, J. Woodley, G. Houin, Gastrointestinal absorption of drugs: methods and studies, Fund. Clin. Pharmacol. 13 (1999) 154–168.
[34] J.R. Campos, A.R. Fernandes, R. Sousa, J.F. Fangueiro, P. Boonme, M.L. Garcia, A.M. Silva, B.C. Naveros, E.B. Souto, Optimization of nimesulide-loaded solid lipid nanoparticles (SLN) by factorial design, release profile and cytotoxicity in human Colon adenocarcinoma cell line, Pharmaceut. Dev. Technol. 24 (2019) 616–622.
[35] N. Passerini, B. Albertini, B. Perissutti, L. Rodriguez, Evaluation of melt granulation and ultrasonic spray congealing as techniques to enhance the dissolution of praziquantel, Int. J. Pharm. 318 (2006) 92–102.
[36] A. zur Mühlen, C. Schwarz, W. Mehnert, Solid lipid nanoparticles (SLN) for controlled drug delivery–drug release and release mechanism, Eur. J. Pharm. Biopharm. 45 (1998) 149–155.
[37] E. Souto, S. Wissing, C. Barbosa, R. Müller, Development of a controlled release formulation based on SLN and NLC for topical clotrimazole delivery, Int. J. Pharm. 278 (2004) 71–77.
[38] F. Kolenyak-Santos, C. Garnero, R.N. de Oliveira, A. de Souza, C. Chorilli, S.M. Allegretti, M.R. Longhi, M.V. Chaud, M.P. Gremião14, Nanostructured lipid carriers as a strategy to improve the in vitro schistosomiasis activity of praziquantel, J. Nanosci. Nanotechnol. 14 (2014) 1–12.
[39] R. Salehzadeh, R. Abdullah, Solid lipid nanoparticles as new drug delivery system, Int. J. Biotechnol. Mol. Biol. Res. 2 (2011) 252–261.
[40] P.M. Cupit, C. Cunningham, What is the mechanism of action of praziquantel and how might resistance strike? Future Med. Chem. 7 (2015) 701–705.
[41] S.-h. Xiao, J.-y. Mei, P.-y. Jiao, The in vitro effect of mefloquine and praziquantel against juvenile and adult Schistosoma japonicum, Parasitol. Res. 106 (2009) 237–246.
[42] S. Martins, S. Costa-Lima, T. Carneiro, A. Cordeiro-da-Silva, E. Souto, D. Ferreira, Solid lipid nanoparticles as intracellular drug transporters: an investigation of the uptake mechanism and pathway, Int. J. Pharm. 430 (2012) 216–227.
[43] C.S. Ferreira Marques, P. Rezende, L.N. Andrade, T.M.F. Mendes, S.M. Allegretti, C. Bani, M.V. Chaud, M. Batista de Almeida, E.B. Souto, L. Pereira da Costa, P. Severino, Solid dispersion of praziquantel enhanced solubility and improve the efficacy of the schistosomiasis treatment, J. Drug Deliv. Sci. Technol. 45 (2018) 124–134.
[44] X.-Y. Ying, D. Cui, L. Yu, Y.-Z. Du, Solid lipid nanoparticles modified with chitosan oligosaccharides for the controlled release of doxorubicin, Carbohydr. Polym. 84 (2011) 1357–1364.